Energy Equip. Sys./ Vol. 13/No. 4/December 2025/ 455-473

ENERGY EQUIPSYS

Energy Equipment and Systems

www.energyequipsys.com

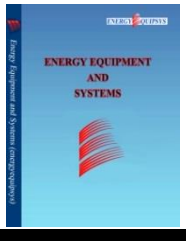

Dynamic simulation and life cycle assessment of a solar water heating system for various commercial and institutional buildings

Authors

Mahsa Khavari[a*]
Farzad Veysi[b]

[a] School of Mechanical Engineering, Iran University of Science and Technology, Tehran, Iran

[b] Mechanical Engineering Department, Faculty of Engineering, Razi University, Kermanshah, Iran

Article history:

Received: 1 August 2025
Revised: 8 September 2025
Accepted : 24 September 2025

ABSTRACT

In this paper, the forced circulation solar water heater system (SWHS) with evacuated tube collectors is dynamically simulated for application in various institutions and commercial buildings While most studies rely on simplified or residential consumption profiles, this research employs distinct, real-world hot water consumption profiles (HWCPs) from ASHRAE standards for different building types (elementary school, restaurant, motel, dormitory) to address a critical gap in system optimization for commercial applications. The presented model is validated, and a parametric study is conducted to investigate the effect of HWCP on the optimum values of system design parameters such as the collector mass flow rate, storage tank volume, and collector area. Moreover, a life cycle assessment (LCA) is conducted to evaluate the impact of HWCPs on financial performance. The findings indicate that by applying the HWCP, which closely resembles the variation in solar radiation observed on an hourly scale, the highest annual solar fraction of the system would be achieved at a lower ratio of tank volume to collector aperture area. On the other hand, due to the low solar radiation from 6 to 10 AM, besides the storage tank's thermal loss overnight, the required auxiliary energy increases for the profiles that allocate a large amount of hot water consumption into these hours. For all different buildings, the highest annual solar fraction is achieved for the collector flow rates of 14 and 15 kg/hm². Moreover, changing the profiles can increase the annual life cycle savings about 31%.

Keywords: Hot Water Consumption Profile; Life Cycle Assessment; Forced Circulation Solar Water Heater System; Evacuated Tube Collector.

1. Introduction

Today, due to the increase in energy demand, the end of fossil fuels, and the negative environmental impacts associated with fossil fuel combustion, the adoption of solar energy and other renewable energy sources appears to be inevitable. Buildings play a significant role in energy consumption and greenhouse gas emissions [1], with around 19% of their total energy consumption dedicated to water heating, especially in subtropical regions [2]. Therefore,

* Corresponding author: Mahsa Khavari
School of Mechanical Engineering, Iran University of Science and Technology, Tehran, Iran
Email: mahsa_khavari@mecheng.iust.ac.ir

by using Solar Water Heater Systems (SWHS), the storage of fossil fuels would be increased, and besides, the air pollution would be decreased. Using SWHS in buildings such as, hotels, restaurants, student dormitories and hospitals, where the hot water consumption is high each day, is more prominent.

According to the type of water circulation in the system, SWHSs can be divided into two main groups: Thermosyphon (natural circulation) and forced circulation [3]. Forced circulation systems are appropriate for applications in cold climates with a high demand for hot water. The solar collectors are the most important part of these systems and have various types, including Flat Plate Collectors (FPC) and Evacuated Tube Collectors (ETC), which are widely used for heating water in small-scale applications [4]. So far, various studies have been conducted on the efficiency of these collectors in heating water [5-7]. Due to the high efficiency, simple structure, low production and maintenance costs, and adaptation to different climatic conditions, ETCs have been investigated widely by many researchers. The conduction and convection losses have decreased in these types of collectors because of vacuum envelope between the internal and external tubes, and so, in the unfavorable environmental conditions, the thermal efficiency of the vacuum tube collectors is higher compared to the efficiency of flat plate collectors [8] .In addition, ETCs can track the sun's movement passively during the day because of their tubular structure [9].

Proper dimensioning of components and the exact prediction of the solar energy delivered to the load is essential for the effective operation of an SWHS. Determining the optimum values of system design parameters as well as evaluating the effect of various operating conditions on the thermal and economic performance of the system, has sparked interest among various researchers. For example, Bani Yaseen et al. [10] studied a natural circulation SWHS and found that flow rate and tilted solar radiation significantly affect system performance, with a peak efficiency of 55% and maximum useful heat gain of 304.81 MJ. Shboul et al. [11] introduced a building-integrated solar thermal photovoltaic system (BIPV/T) for residential buildings to minimize energy consumption. The system's performance was analyzed under different seasonal conditions with a focus on thermal and electrical generation. The system achieved a thermal power output of 5320 W, with a total efficiency of 63%. Recent advancements have introduced more sophisticated dynamic simulation methods based on updated standards (e.g., EN 15316:2017 series) for hourly calculation of system performance and cost-optimal analysis, highlighting significant inaccuracies in older, simplified monthly methods [12]. In addition, the study on the optimum size of SWHSs has been conducted in some papers; for instance, Alsadi et al. [13] examined the optimization of working fluid mass flow rate in SWHS by evaluating not only energetic and economic criteria, but also the auxiliary energy required to meet thermal demands. He found the optimal mass flow rate for a solar flat-plate collector to be 29 kg/h per m² of collector area. Asaee et al. [14] investigated the effects of collector area and storage tank volume on the system solar fraction. In another study [15], using dynamic simulation of SWHS, the criteria for designing the storage tanks for hot water in apartment buildings were proposed. Furthermore, beyond sizing, accurately modeling system behavior—including pump control strategies and the risk of stagnation under high temperatures or low demand—is crucial for realistic performance assessment, as demonstrated in studies extending these standard methods [16].

Life Cycle Assessment (LCA) is among the most commonly applied methods for evaluating environmental impacts globally [17]. Khargotra et al. [18] conducted a technical and economic assessment of a modified solar thermal system. The technical and financial capabilities of the forced circulation SWHS with FPCs for a hospital were studied using a numerical simulation in reference [19] and an economic analysis was performed using the LCA. It was reported that the maximum annual life cycle saving and the maximum collector efficiency were achieved for the collector mass flow rate of 11 kg/h m^2 and a ratio of the tank volume to the collector area of 56 l/m^2. Rezapour et al. [20] performed a dynamic and economic simulation of SWHS to supply domestic hot water in 47 residential locations across Iran. The results indicated an annual solar heat production

of 223.1 MWh, with an average heating cost of 0.160 $/kWh. For industrial applications, Hassan et al. [21] developed a validated numerical model in MATLAB for an Evacuated Flat Plate Collectors (EFPCs) system, highlighting its economic viability with a payback period of 7.4 years for a case study in the textile industry, which is significantly lower than traditional FPC and ETC systems. Elnaggar et al. [22] evaluated the use of solar water heaters in Gaza, showing that this system can significantly reduce annual energy costs up to $3461 with payback periods of 4.4 years. Herrando et al. [23] conducted a comprehensive LCA for a solar combined cooling, heating, hot water, and power (S-CCHP) system, showing that this innovative system has up to 50% lower environmental impacts compared to grid-based systems. Cruz et al. [24] assessed the technical and economic potential of SWHS in Brazilian households. The most critical factors influencing the technical and economic feasibility of these systems were identified as installation cost, household size, and energy prices. A recent study [2] showed that ETC-based SWHS outperformed FPC-based SWHS in a student hostel in India, meeting 67.6% of hot water demand, with a shorter payback period and greater CO_2 emission reductions. It should be noted that all of the above-mentioned studies were carried out for a specific Hot Water Consumption Profile (HWCP).

HWCPs are required for designing SWHSs and estimating the energy consumption. Several factors affect these profiles in buildings, including building usage, number of inhabitants and their presence hours, etc. So far, various studies have been done to estimate the hot water consumption [25-27]. For example, Sousa [28] proposed a dynamic model to estimate hot water consumption and its related energy use, showing that domestic hot water usage varies with season, user behavior, and water temperature, and can be a major energy load in efficient buildings. In addition, some investigations have been conducted to evaluate the effect of HWCPs on the performance of solar water heater systems. For example, Shirinbakhsh et al. [29] studied the influences of daily hot water demand and hourly consumption profile of hot water on the overall performance of SWHSs. The results showed that by increasing the amount of hot water consumed daily, the effect of these profiles becomes more intense. Moreover, daily hot water demand has a significant effect on non-uniform profiles. Mamouri et al. [30] specified the experimental equations to determine the optimal area of ETCs for various heating purposes and different buildings. The control strategies of hot water tank thermal performance using three consumption profiles were investigated by Nkwetta et al. [31]. In another research [32], the solar fraction of the domestic SWHS was evaluated for different HWCPs and the results showed that by applying the profile, which concentrates hot water consumption during the day uniformly, more solar fraction can be achieved compared to the one, which concentrates hot water consumption during the night uniformly. In another study [33], it was shown that approximately 13 kWh/year can be saved for ETC of auxiliary energy by adapting the consumption profile. Khavari et al. [34] showed that aligning hot water usage with solar radiation patterns can reduce the payback period by up to 18% for SWHS with flat plate collectors and 15% for SWHS with evacuated tube collectors. Shafieian et al. [35] examined hot water consumption patterns in Perth households with one, two, and four occupants over a year. In summer, the heat pipe SWHS met almost all of the hot water demand (99%), while in winter, this contribution decreased to 36–51%. Their results indicated that the solar system was most effective in households with higher occupancy, due to increased hot water demand. Furthermore, parametric and optimization studies continue to highlight the critical influence of system design and local conditions on SWHS performance. For instance, Gambade et al. [36] conducted a parametric analysis on an ETC-based system for an agricultural application, demonstrating the significant impact of location and collector orientation. Similarly, Zukowski and Jezierski [37] developed a deterministic mathematical model to predict the useful energy output of medium-sized SDHW systems across three European climates, underscoring that optimal values of key parameters like storage volume are highly climate-dependent. In addition, Oye et al. [38] conducted a holistic modelling and

parametric study of a bathroom SWHS, emphasizing that integrated system design and load profiles play a decisive role in energy savings and CO_2 reduction.

Despite this body of research, a critical literature gap remains. Specifically, the majority of previous studies have focused on residential buildings, where HWCPs are highly influenced by family lifestyle, occupancy patterns, and climatic conditions. Consequently, these profiles are often simplified and do not accurately represent the distinct, high-demand, and scheduled patterns inherent to various commercial and institutional buildings (e.g., schools, restaurants, and dormitories). Furthermore, the interplay between these unique commercial HWCPs and the optimal economic sizing of the system (collector area, tank volume) via Life Cycle Assessment has not been comprehensively explored for forced-circulation ETC systems across multiple building types.

Therefore, the main motivation of this paper is the appropriate and economical design of SWHSs in various institutions and commercial buildings. The novel contribution of this work is twofold: (1) to perform a comparative analysis of the thermal and economic performance of a SWHS under five distinct, real-world HWCPs specific to commercial operations, and (2) to uniquely determine how each profile dictates the optimal values of key design parameters (collector flow rate, storage tank volume, and collector area) to maximize both solar fraction and annual life cycle savings. The dynamic model, which represents the forced-circulation SWHS with ETCs is developed in the SIMULINK program [39]. For different buildings with their specific HWCPs, the optimal values of the collector mass flow rate and tank volume are determined for achieving the appropriate thermal performance of the system. Also, the optimal collector area is evaluated for attaining the highest economic performance using the LCA. Moreover, the effects of HWCPs on the thermal and economic performance of SWHSs are investigated.

Nomenclature

A	surface area, m^2
$ALCS$	annual life cycle savings, USD$
$ALCC$	annual life cycle costs, USD$
C_c	solar collector cost, USD$/$m^2$
C_{fuel}	fuel specific cost, USD$/J
C_s	storage tank cost, USD$
C_p	specific heat, J/kg°C
CRF	capital recovery factor
d	discount rate
i	inflation rate
f	solar fraction
F_R	heat removal factor
I	global irradiation, W/m^2
K_θ	incidence angle modifier
$\dot{m}$	mass flow rate, kg/s
n	time period, years
n_p	payback time, years
PWF	present worth factor
Q	energy, J
$\dot{Q}_{aux}$	auxiliary energy rate provided by the boiler, W
$\dot{Q}_{sol}$	solar energy rate delivered to load, W
$\dot{Q}_u$	useful energy rate gained by the collector, W
t	time, s
T	temperature, °C
U	overall heat loss coefficient, W/°C m^2
V	Volume, m^3

Greek letters

ε	heat exchanger effectiveness factor
η	energy efficiency
ρ	fluid density, kg/m^3
$(\tau\alpha)_n$	transmittance-absorptance product

Subscripts

a	ambient
apr	collector aperture area
aux	auxiliary system
b	boiler
c	Collector
conv	conventional system
f	fluid in the collector loop
i	collector inlet
l	load
m	makeup water
o	collector outlet
s	storage tank
sol	solar system
t	tilted surface

Abbreviations

SWHS	solar water heater system
FPC	flat plate collector
ETC	evacuated tube collector
HWCP	hot water consumption profile
LCA	life cycle assessment
LCS	life cycle savings

2. Simulation procedure

2.1. System description

As depicted in Fig. 1, the system being examined operates based on an indirect forced circulation solar water heating mechanism. The system aims to heat water from an initial temperature of 10 °C up to at least 55 °C. The system consists of evacuated tube collectors arranged in series, a solar pump, a hot water storage tank with a spiral heat exchanger, a gas boiler, and pump controllers. In this system, a heat pipe-type evacuated tube collector has been employed, and their standard test information is provided by the Solar Rating and Certification Corporation [40]. The working fluid is water; if the temperature difference between the collector outlet and the storage tank falls below 10 °C, the pump will shut off [3]. The detailed description of the system components is provided in Table 1.

2.2. Weather data

Dynamic simulation is performed based on the weather conditions of Kermanshah at a latitude of 34.32°N and a longitude of 47.1°E. For each month, one day is considered as a sample. In each sample day, hourly solar radiation incident on the collector surface is calculated using the equations proposed by [3]. Figure 2 shows the monthly mean values of incident solar radiation in Kermanshah according to the simulation results. The hourly ambient temperatures are calculated according to the relations proposed by [42].

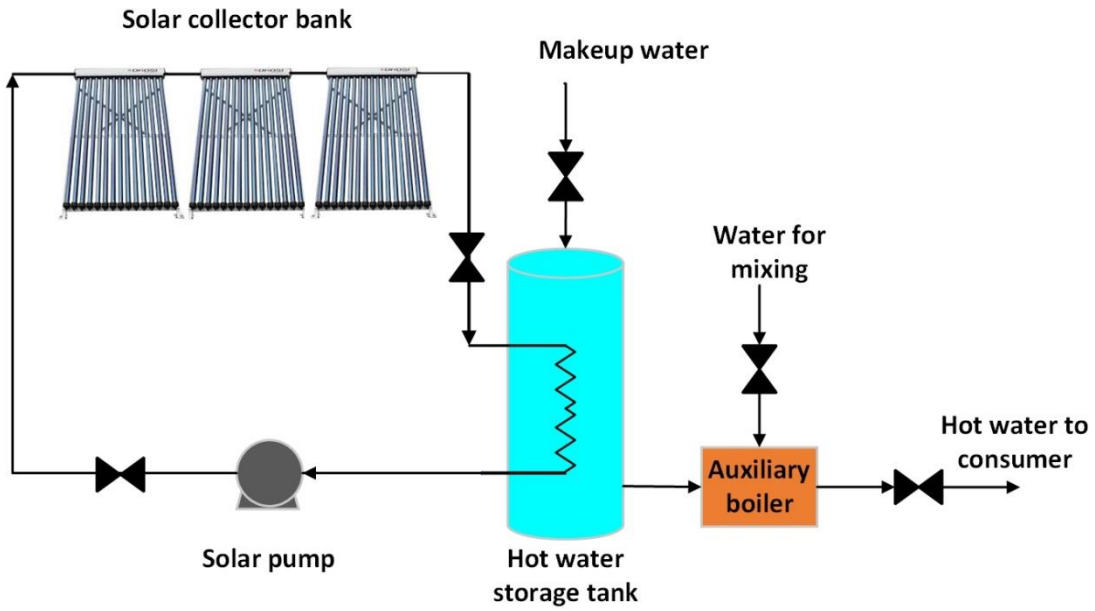

Fig. 1. Schematic diagram of the forced circulation solar water heater system.

Table 1. Technical specifications of solar water heater system components.

Parameter	Unit	Value
$F_R(\tau\alpha_n)$	-	0.426
F_RU_L	w/m^2°C	1.254
Collector gross area	m^2	4.078
Collector net aperture area	m^2	2.308
Number of collectors	-	1-7
Boiler efficiency	-	0.85
Tank heat loss coefficient	w/m^2°C	0.8
Heat exchanger effectiveness factor	-	0.85
Collector tilt angle	Degree	34.32
Collector test flow rate	kg/m^2 s	0.021

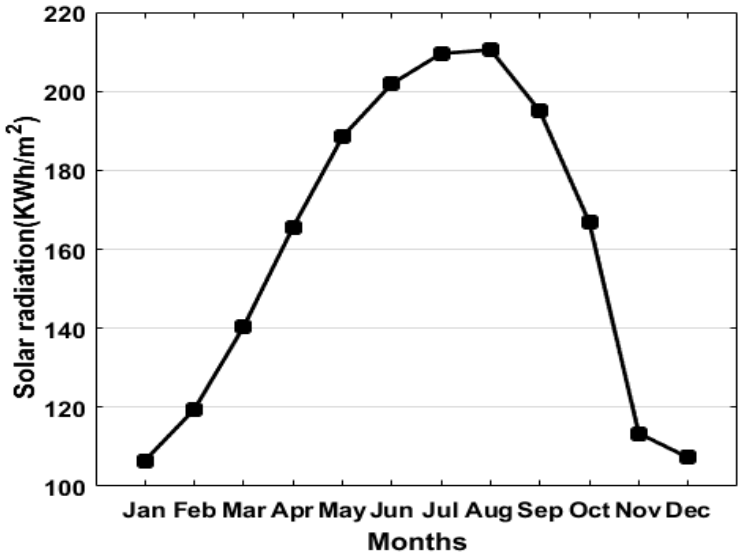

Fig. 2. Average monthly solar radiation values generated by simulation in Kermanshah.

2.3. Hot water consumption profiles

Several factors can influence the hot water consumption profile in buildings. However, the difference between consumption profiles of various commercial buildings with the same application is less than the difference between the profiles of various residential buildings. Therefore, in this study, four profiles are used for different commercial buildings and institutions based on ASHRAE standard [43] with the same daily water consumption of 490 liters, including 1) elementary school, 2) food service restaurant, 3) motel and 4) men's dormitory. These profiles were measured according to the actual tests for sample buildings [43]. The other studied profile (profile 5) shows a uniform hot water consumption with a daily usage of 490 liters. Although Profile 5 (uniform) is rare in practice, it is included herein as a theoretical baseline to provide a clear contrast for evaluating the impact of temporally varying demand patterns on system performance. Figure 3 depicts all profiles, and Table 2 summarizes the key characteristics of the hot water consumption profiles shown in Fig. 3.

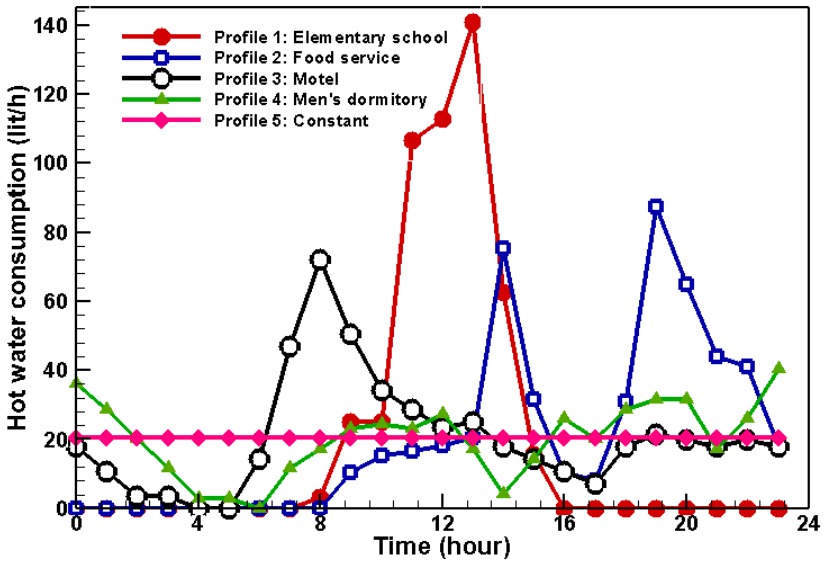

Fig. 3. Hourly hot water usage profiles applied in the simulation [43].

Table 2. The main features of the hot water consumption profiles presented in Fig. 3.

Profile	Building type	Daily consumption (Liters)	Peak demand hours	Notable Pattern / Justification
1	Elementary school	490	1 PM	Single, sharp midday peak. Aligns with lunchtime and cleaning.
2	Restaurant	490	2 PM, 7 PM	Twin peaks aligned with lunch and dinner service hours.
3	Motel	490	8 AM	Strong morning peak due to guests showering/checking out.
4	Men's Dormitory	490	7 AM, 7 PM, 11 PM	Multiple peaks (morning showers, evening leisure, night).
5	Uniform (Baseline)	490	Uniform	Constant demand throughout the day (theoretical benchmark).

3. Mathematical modeling of the system

3.1. Modeling of the solar collector

The dynamic simulation of the forced-circulation solar water heater system is carried out in this paper. For this purpose, system components such as collectors and storage tank should be modeled. The efficiency of solar collector (η_c) is calculated by Eq. (1) [3]:

$$\eta_c = F_R(\tau\alpha)_n K_\theta - F_R U_L \left(\frac{T_i - T_a}{I_t}\right) \quad (1)$$

where K_θ is the incidence angle modifier that is provided by the collector testing institute [40]. I_t is the solar flux reaching the collector surface, T_a is the surrounding temperature and T_i is the collector inlet fluid temperature. In this study, the collector parameters, $F_R(\tau\alpha)_n$ and $F_R U_L$, which are listed in Table 1, are calculated based on the collector gross area that is the total surface occupied by collector. These parameters are modified to determine the variation between the water flow rate during testing and the flow rate applied in actual conditions [3].

The rate of useful energy gained by the collector is determined using Eq. (2) [3,41]:

$$\dot{Q}_u = A_c I_t \eta_c = \left(A_c I_t K_\theta F_R(\tau\alpha)_n\right) - \left(A_c F_R U_L (T_i - T_a)\right) \quad (2)$$

where A_c is the collector gross area.

3.2. Modeling of the hot water storage tank

In the modeling of a storage tank, the temperature distribution of fluid in the tank is assumed to be fully mixed. Considering proper insulation of pipes and fittings, the heat losses from these parts can be ignored. The energy equilibrium equation for the storage tank is presented in Eq. (3) [3, 41]:

$$\dot{m}_f C_p (T_o - T_i) - \dot{m}_l C_p (T_s - T_m) - U_s A_s (T_s - T_a) = \rho C_p V_s \frac{dT_s}{dt} \quad (3)$$

where T_m is the cold water temperature entering the storage tank (°C), which is equal to 10 °C in this work, T_s is the hot water temperature inside the tank, T_o is the collector outlet fluid temperature, A_s is the surface area of the tank and U_s is the overall heat loss coefficient of the tank. In addition, $\dot{m}_f$ is the collector mass flow rate (kg/s) and $\dot{m}_l$ is the hot water mass flow rate demanded by the load. C_p is the water specific heat (J/kg. °C), ρ is the water density (kg/m^3) and V_s is the tank volume (m^3). The first, second, and third terms on the left side of Eq. (3) are the energy transfer rate from collectors to the storage tank, the energy transfer rate from the solar water heater system to the load, and the heat loss rate from the storage tank, respectively. By defining the heat exchanger effectiveness factor of the tank (Eq. (4) [3, 41]), the Eq. (3) is rewritten in the form of Eq. (5):

$$\varepsilon = \frac{T_o - T_i}{T_o - T_s} \quad (4)$$

$$\dot{m}_f C_p \varepsilon (T_o - T_s) - \dot{m}_l C_p (T_s - T_m) = \rho C_p V_s \frac{dT_s}{dt} \quad (5)$$

3.3. Modeling of the system thermal performance

In the present study, the thermal performance is determined using the solar fraction of the system, which is defined as the fraction of energy demanded by the load that is provided by

solar energy, and can be calculated by Eq. (6) [3, 41]:

$$f = \frac{\dot{Q}_{sol}}{\dot{Q}_{sol} + \dot{Q}_{aux}} \quad (6)$$

where $\dot{Q}_{sol}$ is the solar energy rate delivered to the load and $\dot{Q}_{aux}$ is the auxiliary energy rate provided by the boiler and can be computed by Eqs. (7) and (8), respectively.

$$\dot{Q}_{sol} = \dot{m}_l C_p (T_s - T_m) \quad (7)$$

$$\dot{Q}_{aux} = \frac{1}{\eta_b}[m_l C_p (T_l - T_s)] \quad (8)$$

where T_l is the minimum hot water temperature demanded by the load, which is equal to 55 °C in this study, and η_b is the boiler efficiency.

By integrating the four main component blocks—the collector, storage tank, heat exchanger, and boiler—the overall system block diagram is constructed. The system is solved iteratively by linking the outlet fluid temperature from the collector block to the tank input and the outlet fluid temperature from the internal heat exchanger back to the collector input. After several iterations with initial guesses for the tank temperature and energy values, the solution converges to acceptable results. The system's solar fraction, required auxiliary energy, and solar energy rate delivered to the load are computed as the primary outputs for different time periods. The overall simulation block diagram is shown in Fig. 4. The modeling sequence is as follows:

- **Collector Block:** Inputs: hourly ambient temperature, solar radiation, and collector inlet fluid temperature. Using Eqs. (1) and (2), it calculates the collector outlet temperature.
- **Storage Tank Block:** Inputs: make-up water temperature, collector outlet temperature, ambient temperature. Using the energy balance equations (Eqs. 3 and 5) and the specific HWCP, it calculates the hourly storage tank temperature and the solar energy delivered to the load.
- **Heat Exchanger Block:** Inputs: collector outlet temperature and hot water temperature inside the tank. Using Eq. (4) (effectiveness), it calculates the heat exchanger outlet temperature, which is fed back as the collector inlet temperature.
- **Boiler Block:** Inputs: current hot water temperature inside the tank and the defined set-point temperature. Using Eq. (8), it calculates the auxiliary energy required to heat the water from the storage tank temperature to the set-point.

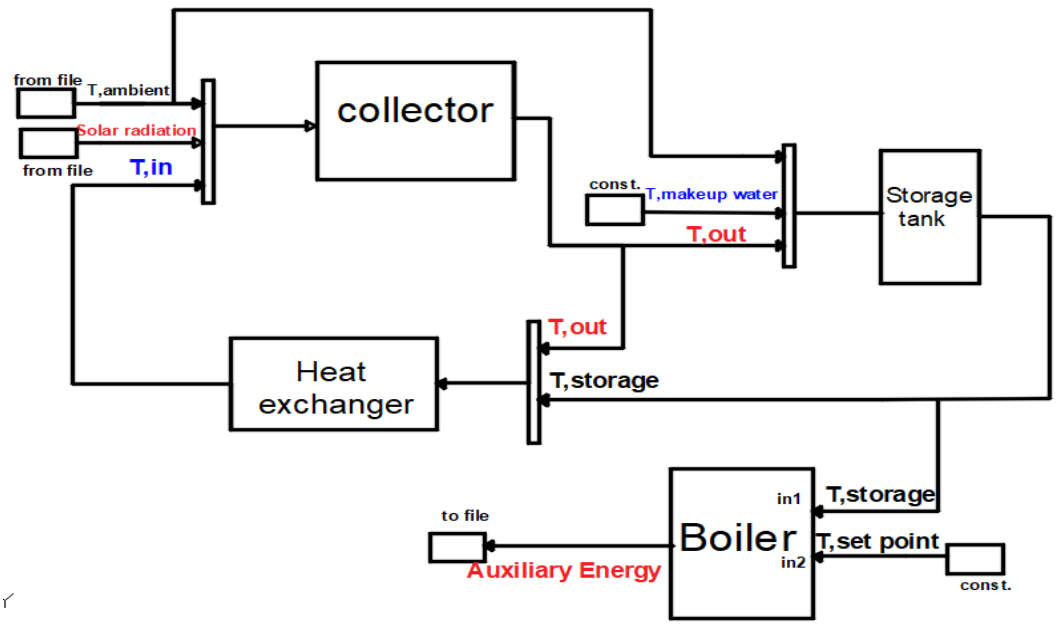

Fig. 4. Block diagram of the overall modeled solar water heating system.

4. Economic analysis

In this paper, the LCS method is used for financial analysis [3,41]. The economic performance of the system is determined based on the Annual Life Cycle Savings (ALCS), which refers to the difference between the Annual Life Cycle Cost (ALCC) of the solar energy system and the conventional fuel system. according to Eq. (9):

$$ALCS = ALCC_{conv} - ALCC_{sol} \quad (9)$$

The $ALCC$ for the conventional system and solar system can be calculated by Eqs. (10) and (11), respectively:

$$ALCC_{conv} = Q_l \; C_{fuel} \; PWF\left(i;d;n\right)CRF \quad (10)$$

$$ALCC_{sol} = \left[\left(C_s + A_c C_c\right).CRF\right] + \left[0.03\left(C_s + A_c C_c\right).PWF\left(i;d;n\right).CRF\right] + \left[Q_{aux} C_{fuel}.PWF\left(i;d;n\right).CRF\right] \quad (11)$$

where Q_l is the annual energy required for heating water through the fuel combustion, Q_{aux} is the annual auxiliary energy provided by the boiler in the SWHS, C_{fuel} is the fuel-specific cost, C_s and C_c correspond to the costs of the storage tank and solar collector, respectively. The present worth factor $PWF(i;d;n)$, which is defined by Eq. (12), is used to convert the costs of the solar system at the end of the first year into the sum of inflated costs during n years according to the present worth of money. Eq. (13) is used to calculate the capital recovery factor (CRF), which distributes the present worth of costs over the period of n years into equal and uniform payments [3, 41].

$$PWF\left(i;d;n\right) = \frac{1}{d-i}\left[1-\left(\frac{1+i}{1+d}\right)^n\right] \quad (12)$$

$$CRF = \frac{d\left(1+d\right)^n}{\left(1+d\right)^n - 1} \quad (13)$$

where i is the inflation rate and d is the market discount rate. The terms on the right side of Eq. (11) represent the initial purchase cost of the solar system equipment, the maintenance cost that is assumed to be 3% of the initial purchase cost of the equipment [44] with an inflation rate of 1% per year, and the cost of supplying fuel for the auxiliary system (gas boiler), respectively. The boiler is assumed to be identical in both solar and conventional fuel systems, so, the boiler cost can be ignored in the calculation of $ALCS$.

The system payback time (n_p) is the time needed for the cumulative fuel savings to become equal to the total initial investment and can be computed by solving Eq. (14) [3]:

$$\dot{Q}_{sol} C_{fuel} PWF\left(n_p.i.d\right) = \left(C_s + A_c C_c\right) \quad (14)$$

The economic parameters used are listed in Table 3.

Table 3. Economic parameters.

Parameter	Unit	Value
Discount rate (%)	%	10
Inflation rate (%)	%	9
Life cycle	years	20
Solar collector cost	USD$/m^2	150
Thermal storage cost	USD$/m^2	84.2 [45]
Fuel cost	USD$/m^3	0.5

5. Model validation

In order to validate the developed model, the simulation results obtained in this study are compared with the experimental results presented in reference [5]. For this purpose, the same technical specifications and operating conditions as the studied system in reference [5] are considered for the SWHS, and then, the system is simulated. The total heat delivered to the load by the SWHS is calculated for three different days and the results are compared with the measured values. According to reference [5], in order to characterize different weather conditions in Ireland, simulations are performed for three days, including clear sky in summer (02/06/2009), intermittent cloud cover in autumn (25/11/2009), and heavily overcast in winter (20/1/2010). Figure 5 shows the variations of measured and modelled heat delivered to the load by SWHS during the mentioned three days. As it is obvious from this figure, the predictions by the proposed model follow a similar trend as the measured heat delivered to the load; however, in all three days, a mean overestimation error of 7.5% is observed for the heat delivered to the load. This level of discrepancy (7.5%) is considered acceptable for dynamic simulations of solar thermal systems and is consistent with the range of errors reported in the benchmark study [5]. The differences between the simulation and experimental results are

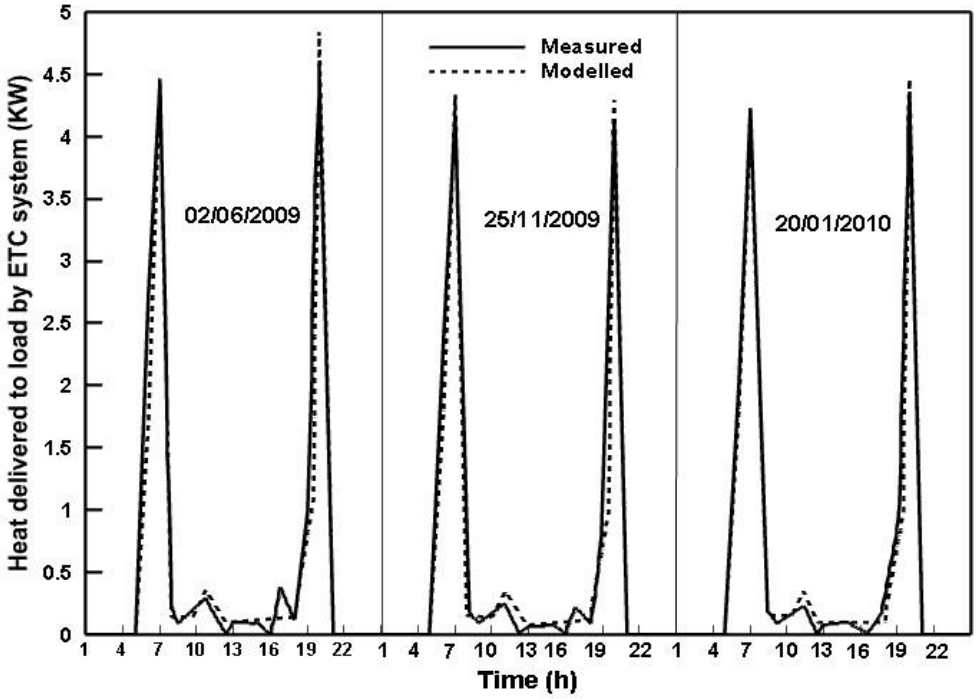

Fig. 5. Measured and modelled heat delivered to load by SWHS.

primarily due to the uniform temperature distribution of water inside the tank and the omission of thermal losses in the pipes within the developed model.

6. Results and discussion

6.1. Parametric study of the solar water heater system

In order to determine the proper size of the system, a parametric study must be performed. For this purpose, the initial system is considered to be the starting point of the simulations and its design parameters are chosen based on the collector manufacturer's recommendation and technical literature. According to the collector standard test information [40], each of the evacuated tube collectors used in the simulation produces an average of 3146.1 kWh per year. In this work, in order to increase the water temperature to 55 °C, an average amount of 9295.6 kWh per year would be required. By dividing the annual energy requirement for water heating by the annual energy generated by each collector, the number of collectors required to simulate the initial system would be achieved, which is equal to three (or a collector gross area of 12.2 m^2). In addition, for this system, the ratio of the storage tank volume to the collector's net aperture area (V_s/A_{apr}) is assumed to be 50 l/m^2 [3]. The initial system is simulated for different values of design parameters, so that the optimum size of the system can be determined. In the present study, the optimum values of collector flow rate and tank volume are those that maximize the annual solar fraction (*f*), and the optimum value of collector area is the one at which the maximum $ALCS$ is achieved.

The initial ranges for the collector mass flow rate (5–50 kg/h•m^2) and storage tank volume ratio (10–100 l/m^2) are selected based on recommendations from prior literature and practical constraints commonly adopted in solar water heating system design. For instance, studies such as [46] and [47] have indicated that flow rates below 5 kg/h•m^2 may lead to insufficient heat extraction and excessive thermal losses, while values above 50 kg/h•m^2 may result in negligible temperature rise across the collector. Similarly, tank volume ratios below 10 l/m^2 are often impractical due to insufficient thermal storage, whereas ratios exceeding 100 l/m^2 are associated with increased thermal losses and higher initial costs without significant gains in solar fraction [15, 3]. These ranges ensure that the parametric study covers both typical operational values and extreme

cases to comprehensively identify optimum design parameters.

6.1.1. Determination of the collector flow rate

In the first step of the parametric study, the initial system is simulated for different ratios of collector flow rate to the collector net aperture area ($\dot{m}/A_{apr}$). Figure 6 shows the variation of annual f against $\dot{m}/A_{apr}$ for various hot water consumption profiles. According to this figure, in all profiles by increasing $\dot{m}/A_{apr}$ from 5 to 14-15 kg/h m^2, a gradual increase of f can be observed. This initial increase occurs because a higher flow rate enhances heat extraction from the collectors, reducing the average collector temperature and thus thermal losses, which improves efficiency. By applying profiles 1, 3, 4 and 5 for a water flow rates of 15-20 kg/h m^2 and by applying the profile 2 for a flow rate of 14 kg/h m^2, the maximum annual f is achieved. With a further increase in $\dot{m}/A_{apr}$ up to 50 kg/h m^2, the decreasing trend is evident in the annual f. This decline is due to the insufficient temperature rise across the collector, which diminishes the useful energy gain. According to the obtained results, the system's operation at the most efficient $\dot{m}/A_{apr}$ can increase the useful energy gained by collectors (Q_u), which leads to an increase in annual f, subsequently. Also, there is a good agreement between the optimum ranges of collector flow rate obtained in this study with those in the previous studies [46-47]. Specifically, the optimal range of 14-15 kg/h.m^2 aligns well with the findings of [46] for similar ETC systems and reinforces the design recommendations provided in [47].

As can be seen from Fig. 6, in all ratios of $\dot{m}/A_{apr}$ Applying profiles 2 and 3 results in the maximum and the minimum annual f, respectively. The difference between the annual solar fraction of system by using these two profiles is on average 8%. It should be noted that in the profile 3, as indicated in Fig. 3, the peak of hot water consumption is at 8AM, when the SWHS is not fully activated due to the low solar radiation, therefore, the system must also provide 41% of the daily hot water demand between 6 and 10 AM, which increases the required auxiliary energy and reduces the thermal performance of the SWHS, consequently. According to Fig. 3, profile 2 has the lowest hot water consumption between 6 and 10 AM which is equivalent to 5% of the daily hot water demand, and the peaks of hot water consumption are at 2 PM and 7 PM (around lunch and dinner times), when the system is more active during these hours. Therefore, by applying profile 2, the auxiliary energy provided by the boiler is reduced and the thermal efficiency of the system is improved.

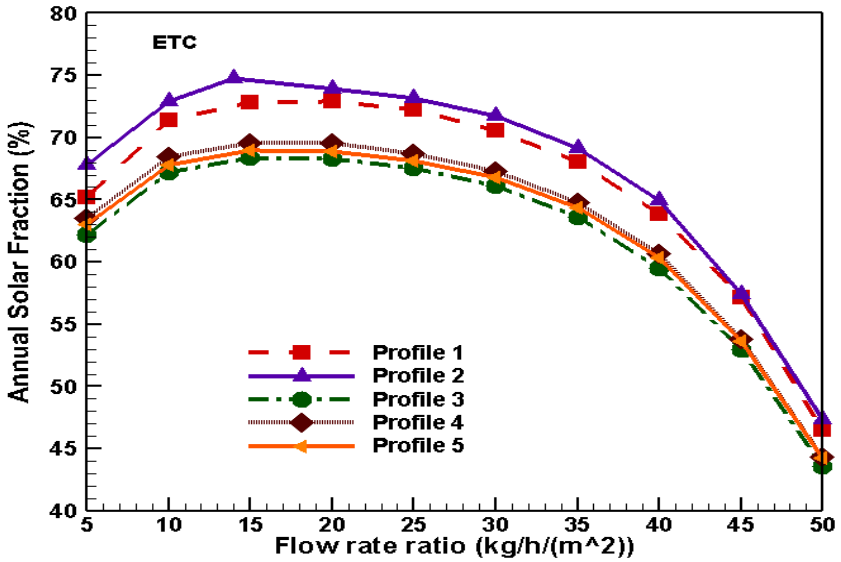

Fig. 6. The annual solar fraction's variation with respect to the ratio of collector flow rate to the collector aperture area ($\dot{m}/A_{apr}$) for various hot water consumption profiles.

Figure 7 shows the variation of the monthly f for the initial system with different profiles by using an optimal collector flow rate of 15 kg/h m^2. According to this figure, the absolute difference between the monthly f values of different profiles is greater for the months with the higher solar radiation (between June and September). In these months, the solar fraction (f) for Profile 1 is, on average, 5% higher than for Profile 2. Furthermore, the largest absolute difference observed between any two profiles was 10.5%, occurring between Profile 1 and Profile 5. Moreover, it can be seen that changing profiles can increase the summer and winter solar fractions up to 10.9% and 9%, respectively.

6.1.2. Determination of the collector area

In the second step of the parametric study, the optimum collector area is determined. The initial system is simulated for different values of the collector gross area using the optimum $\dot{m}/A_{apr}$ that were determined in the first step, i.e. 15 kg/h m^2 for the SWHS with profiles 1, 3, 4 and 5, and 14 kg/h m^2 for the SWHS with profile 2. As expected, increasing the collector area enhances the absorption of solar radiation by the collectors, thus improving the thermal performance of the SWHS. However, the associated increase in initial cost means the economic performance is optimized only when the collector area reaches its specific optimal value. However, the economic performance is optimized only when the collector area reaches its optimal value. Therefore, in this paper, the optimal collector area is determined in such a way that the maximum ALCS is attained. Figure 8 shows the variation of $ALCS$ versus collector gross area. As can be seen in this figure, for all profiles, the $ALCS$ reaches the maximum value when the collector gross area is 12.2 m^2. This result is crucial for system designers, indicating that simply maximizing collector area is not cost-effective; beyond this point, the marginal gain in energy savings does not justify the additional investment. In this case, the SWHSs with profiles 1 to 5 have payback times of 7.1, 7, 8, 7.9, and 7.9 years, respectively. As expected, for all of the investigated collector areas, applying Profile 2 leads to highest thermal performance of the system and maximum $ALCS$. The results show that changing profiles can on average, reduce the system payback time by up to 15% and increase the $ALCS$ by up to 31%.

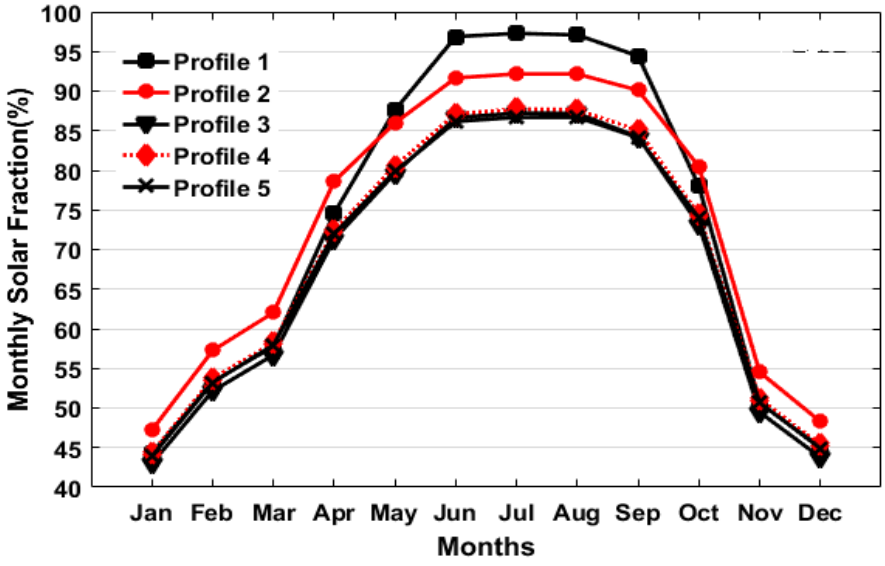

Fig. 7. Monthly solar fraction variation for various hot water consumption profiles.

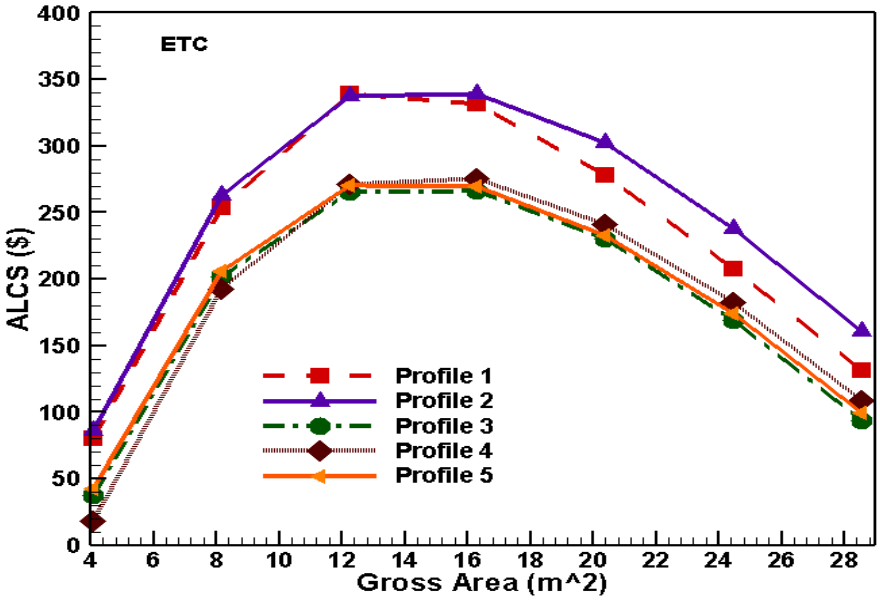

Fig. 8. The change in ALCS with respect to the collector's gross area for various hot water consumption profiles.

6.1.3. Determination of the storage tank volume

In the third step of the parametric study, the system is simulated for different ratios of tank volume to the collector net aperture area (V_s/A_{apr}) using the optimum collector gross area of 12.2 m^2 as well as the values of $\dot{m}/A_{apr}$, which were determined in the first step, i.e. 15 kg/h m^2 for the SWHS with profiles 1, 3, 4 and 5, and 14 kg/h m^2 for SWHS with profile 2. Figure 9 illustrates the variation of the annual f in relation to V_s/A_{apr} for different profiles. According to this figure, for the system with profile 1, the maximum annual f is achieved when the V_s/A_{apr} is in the range of 20 to 35 l/m^2. For the system with profile 2, in the range of 35 to 45 l/m^2, the annual f is around 1% below the highest annual f recorded at a ratio of 50 l/m^2, which is equal to 74.7%. Moreover, for the system with profiles 3, 4 and 5, the appropriate ranges of V_s/A_{apr} are found to be in the range of 30 to 40 l/m^2, 35 to 50 l/m^2, and 35 to 45 l/m^2, respectively. A larger tank volume stores more solar energy for use during non-sunny hours, improving the solar fraction. However, excessively large tanks increase thermal losses and initial cost, leading to the performance decline observed beyond approximately 50 l/m^2. The optimum ratios obtained for V_s/A_{apr} agree with the limits reported in [3] and are consistent with the findings of [15] for commercial buildings, which suggested a range of 30-60 l/m² depending on the climate and load pattern.

As shown in Fig. 9, by applying the tank volumes that are less than 40 l/m^2, the annual f for the system with profile 1 is greater than the annual f for the system with other profiles. As it is evident, by increasing V_s/A_{apr} from 50 to 100 l/m^2, the reduction rate of the annual f for the system with profile 1 is higher compared to the reduction rate of annual f for the system with other profiles. In addition, according to the obtained results, by using profile 1, SWHS achieves the maximum annual f at lower V_s/A_{apr} compared to the other profiles. In other words, for each collector net aperture area, the system with profile 1 needs the smallest tank for improving the thermal performance. According to Fig. 3, at 1 PM, when solar radiation approaches its maximum, profile 1 shows a single peak in hot water consumption, with consumption being concentrated exclusively during the day, and it is almost similar to the hourly variations of solar radiation. As a result, receiving solar energy by the SWHS coincides with consuming hot water by the consumer, and before the end of solar radiation, the hot water consumption reaches zero. Therefore, it can be concluded that for system with profile 1, applying the lower ratio of V_s/A_{apr} could improve the thermal performance. But in other profiles, the hot water is also demanded during

the night and in the morning, when the solar radiation is unavailable or low, so, the system requires a larger tank volume in order to meet the heating demand during the night and early morning.

Figure 9 shows that by increasing the tank volume ratio from 10 lit/m^2 to the mentioned appropriate values, the increase of the annual f is the lowest for profile 1 and equals to 3%, in contrast, it is the highest for profile 4, in which the increase is 17%. The reason is due to the fact that compared to other profiles, in profile 4, the hot water usage is the highest value in the times when solar radiation is unavailable and about 51% of the daily hot water requirement is dedicated to these times. Therefore, the annual f rises quickly as the tank volume grows from 10 l/m^2 to the optimal value. It is also observed that for all profiles, by increasing V_s/A_{apr} from the proposed values to 100 l/m^2, annual f decreases rapidly, because the heat losses from the storage tank increase and hot water temperature in the tank is not sufficient for the heating needs.

Figure 10 shows the hourly variations of the hot water temperature in the storage tank (T_s) on the coldest sample day (17 January) for profiles 2 and 3 in different tank volume ratios. According to Fig. 10 (a) and Fig. 10 (b), by applying the small tank volume (10 l/m^2) when no solar energy is available, a sharp decrease can be seen in storage temperature. Also, it is evident that by using an appropriate tank volume (35 l/m^2) during peak demand hours, storage temperature increases. Moreover, according to Fig. 11 (a), for the system with profile 2, using a tank volume ratio of 35 l/m^2 at 7 PM (time of second consumption peak) can increase the solar energy delivered to the load (Q_{sol}) by 57% compared to the tank volume ratio of 10 l/m^2, and this increase for the system with profile 3 at 8 AM (time of only consumption peak) is equal to 92%, as depicted in Fig. 11 (b). As can be seen from Fig. 11, by using a tank volume ratio of 200 l/m^2, the rise in surface area of the tank and the corresponding increase in thermal losses contribute to a decrease in Q_{sol}. Therefore, it can be understood that using an appropriate tank volume can increase the solar energy delivered to the load during peak demand hours, which leads to an improvement in thermal performance, subsequently.

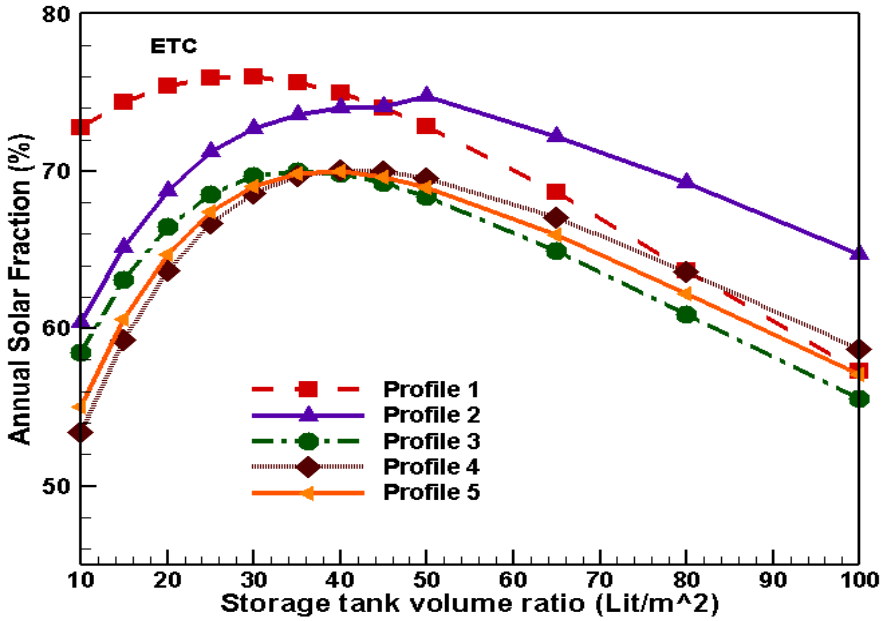

Fig. 9. The fluctuation of the annual solar fraction in relation to the ratio of storage tank volume to collector aperture area (V_s/A_{apr}) for different hot water consumption profiles.

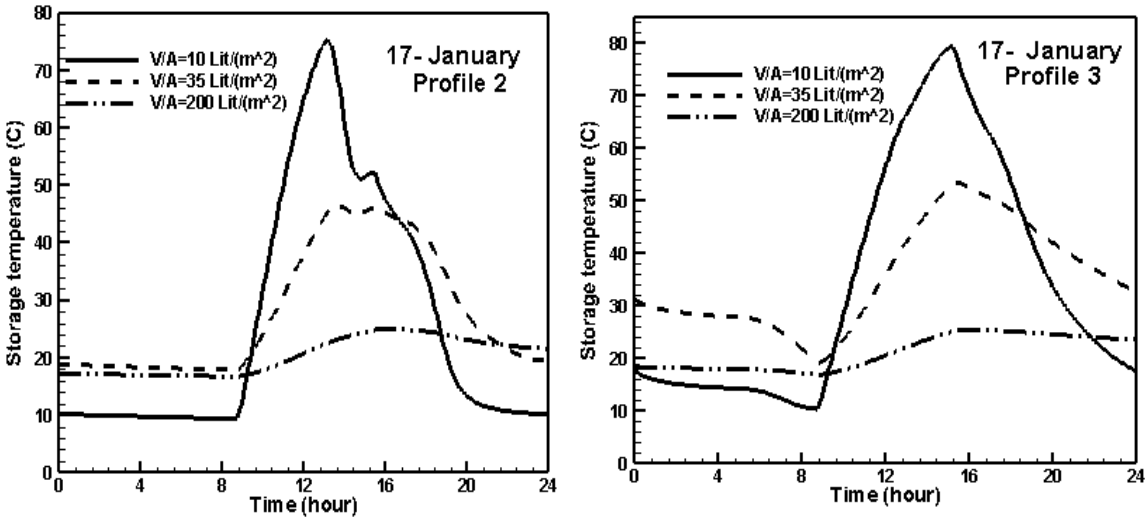

(a) **(b)**

Fig. 10. Hourly variation of the temperature of water stored in the tank on 17th of January for various storage tank volume ratios ($\boldsymbol{V_s/A_{apr}}$) in two cases, (a) use of profile 2, (b) use of profile 3.

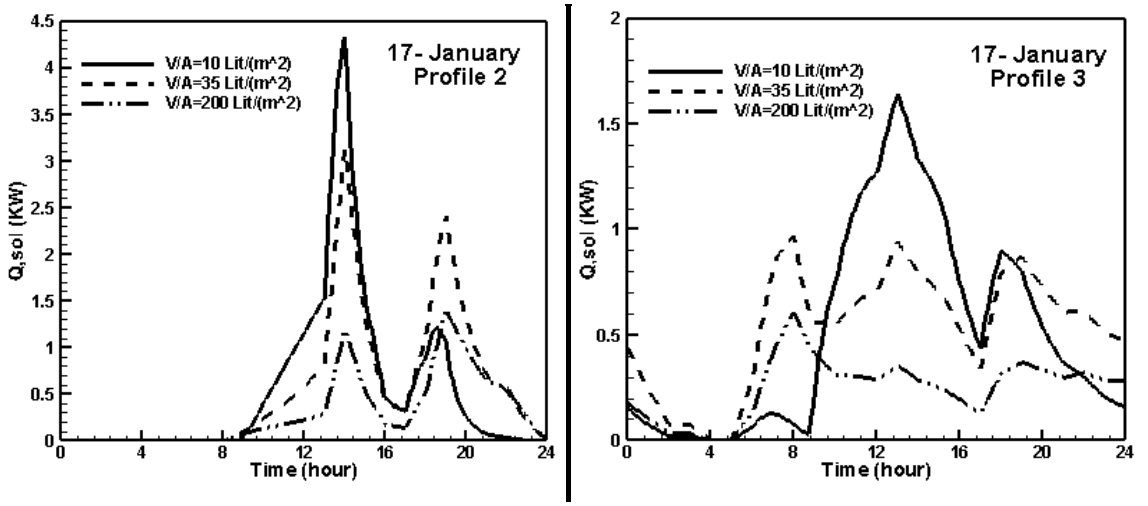

(a) **(b)**

Fig. 11. Hourly variation of the solar energy delivered to the load (Q_{sol}) on 17th of January for various storage tank volume ratios ($\boldsymbol{V_s/A_{apr}}$) in two cases, (a) use of profile 2, (b) use of profile 3.

Finally, in Table 4, the final configurations proposed for the systems studied in this paper are presented. These final configurations show the values of design parameters that lead to the highest thermal and economic performance of the system.

Table 4. Proposed final configuration for SWHSs by using various profiles.

Parameter	Profile 1	Profile 2	Profile 3	Profile 4	Profile 5
Total collectors' gross area (m^2)	12.2	12.2	12.2	12.2	12.2
Total collector's aperture area (m^2)	6.9	6.9	6.9	6.9	6.9
Collector flow rate, (kg/h m^2)	15	14	15	15	15
Storage tank volume ratio, (l/m^2)	25	50	35	40	40
ALCS ($)	374	348	283	276	280
Payback time (years)	6.55	7	7.7	7.8	7.76
Annual solar fraction (%)	76	74.7	70	70.1	69.9

7. Conclusions

This study dynamically simulated and evaluated the thermal and economic performance of a forced-circulation solar water heating system with evacuated tube collectors for various commercial and institutional buildings employing distinct hot water consumption profiles. The main findings are summarized as follows:

- The hot water consumption profile is a critical determinant of both optimal system design and economic viability. When each system is optimally sized for its specific profile, Profile 1 (Elementary School) demonstrates the best overall economic performance, achieving the highest annual life cycle savings (ALCS of 374 $) and the shortest payback period (6.55 years). This is because its consumption is concentrated during midday hours, requiring less storage and minimizing thermal losses, which maximizes solar energy utilization and economic return.
- The optimal collector mass flow rate was consistently identified between 14-15 kg/h•m² for maximizing the annual solar fraction, regardless of the profile type.
- The optimal storage tank volume is highly dependent on the hot water usage profile. Profile 1 (Elementary School), which closely mirrors solar radiation patterns, achieved its highest annual solar fraction with a smaller tank volume (20-35 l/m²). In contrast, profiles with significant morning or evening demand (e.g., Profiles 3 and 4) required a larger tank volume (35-50 l/m²) to store solar energy for later use.
- The optimal collector area for maximizing economic savings (ALCS) was found to be 12.2 m² under the defined economic conditions, consistent across all profiles.
- Significant performance and economic gains are achievable through profile-aware design. Strategically selecting the system design for a specific hot water usage profile can increase annual life cycle savings by up to 31% and reduce the system payback period by up to 15%. In addition, the summer and winter solar fractions can increase up to 10.9% and 9%, respectively.

The results underscore the necessity of using accurate, building-specific load profiles rather than generic assumptions for the optimal design of solar water heating systems in commercial applications. For buildings where hot water consumption can be partially managed—such as through the scheduled operation of washing machines, dishwashers, or cleaning activities—concentrating this controllable demand between 1 PM and 8 PM is recommended. This aligns usage with peak solar radiation, reducing auxiliary energy needs and improving overall system performance. However, for institutions with inflexible schedules, shifting consumption is often impractical. Therefore, the most robust and universally applicable strategy remains the accurate sizing of the system based on the actual, unshifted hot water consumption profile of the building.

References

[1] Zondag H A, de Groot R, van Helden W G J, de Keizer J, van der Veen J. The performance of solar water heaters in the Netherlands: A review of results from a field test. Solar Energy. 2003; 75(3): 239-251.

[2] Duffie J A, Beckman W A. Solar Engineering of Thermal Processes. John Wiley & Sons, New York, 2013.

[3] Kalogirou S A. Solar Energy Engineering-Processes and Systems. Elsevier, 2009.

[4] García-Valladares O, García-Rodríguez L, Juárez-Romero C, Pérez-López J, Vera-Toscano M, Díaz-Hernández F. Thermal performance of a solar water heater with a two-phase thermosyphon. Energy Conversion and Management. 2018; 156: 509-517.

[5] Ayompe L, Duffy A, McCormack S, Conlon M. Validated TRNSYS model for forced circulation solar water heating systems with flat plate and heat pipe evacuated tube collectors. Applied Thermal Engineering. 2011; 31(8-9): 1536-1542.

[6] Mazarrón F R, Porras-Prieto C J, García J L, Benavente R M. Feasibility of active solar water heating systems with evacuated tube collector at different operational water

temperatures. Energy Conversion and Management. 2016; 113: 16-26.
[7] Kumar Y, Shekhar S, Verma M, Ghritlahre H K. Comparative performance analysis of dual spiral and parallel riser tubes in solar flat plate water heater with and without reflector: an experimental study. Journal of Thermal Analysis and Calorimetry. 2025; 1-18.
[8] Upadhyay B, Kumar R, Kovács A, Singh T. Techno-economic analysis of solar thermal collector for sustainable built environment. Journal of Thermal Analysis and Calorimetry. 2024; 149(3): 1175-1184.
[9] Sabiha M, Saidur R, Mekhilef S, Mahian O. Progress and latest developments of evacuated tube solar collectors. Renewable and Sustainable Energy Reviews. 2015; 51: 1038-1054.
[10] Bani Yaseen A, Al-Hyari L, Almahmoud O, Hammad M. Performance of a new solar water heater design with natural circulation. Energy Sources, Part A: Recovery, Utilization, and Environmental Effects. 2024; 46(1): 10694-10709.
[11] Shboul B, Zayed M E, Ashraf W M, Usman M, Roy D, Irshad K, Rehman S. Energy and economic analysis of building integrated photovoltaic thermal system: Seasonal dynamic modeling assisted with machine learning-aided method and multi-objective genetic optimization. Alexandria Engineering Journal. 2024; 94: 131-148.
[12] Patrčević F, Dović D, Horvat I, Filipović P. A Novel Dynamic Approach to Cost-Optimal Energy Performance Calculations of a Solar Hot Water System in an nZEB Multi-Apartment Building. Energies. 2022; 15(2): 509.
[13] Alsadi S, Foqha T. Mass flow rate optimization in solar heating systems based on a flat-plate solar collector: A case study. Renewable Energy Journal. 2021; 60: 215-226.
[14] Asaee S R, Ugursal V I, Beausoleil-Morrison I, Ben-Abdallah N. Preliminary study for solar combisystem potential in Canadian houses. Applied Energy. 2014; 130: 510-518.
[15] Rodríguez-Hidalgo M C, Rodríguez-Aumente P A, Lecuona A, Legrand M, Ventas R. Domestic hot water consumption vs. solar thermal energy storage: The optimum size of the storage tank. Applied Energy. 2012; 97: 897-906.
[16] Piana E. A, Grassi B, Socal, L. A Standard-Based Method to Simulate the Behavior of Thermal Solar Systems with a Stratified Storage Tank. Energies. 2020; 13(1): 266.
[17] Hamidinasab B, Goli A, Shirinbakhsh M, Bahrami M, Mahian O, Mehrabian M, Kowsary M, Alsadi S. Illuminating sustainability: a comprehensive review of the environmental life cycle and exergetic impacts of solar systems on the agri-food sector. Solar Energy. 2023; 262: 111830.
[18] Khargotra R, Kumar R, Kovács A, Singh T. Techno-economic analysis of solar thermal collector for sustainable built environment. Journal of Thermal Analysis and Calorimetry. 2024; 149(3): 1175-1184.
[19] Lima T P, Dutra J C C, Primo A R M, Rohatgi J, Ochoa A A V. Solar water heating for a hospital laundry: A case study. Solar Energy. 2015; 122: 737-748.
[20] Rezapour S, Jahangiri M, Shahrezaie A G, Goli A, Farsani R Y, Almutairi K, Techato K. Dynamic simulation and ranking of using residential-scale solar water heater in Iran. Journal of Environmental Engineering and Landscape Management. 2022; 30(1): 30-42.
[21] Hassan Z, Mahmood M, Ahmed N, Saeed M. H, Khan R, Abbas M. M., Abdelsalam E. Techno-economic assessment of evacuated flat-plate solar collector system for industrial process heat. Energy Science & Engineering. 2023; 11(6): 2185-2201.
[22] Elnaggar M. Useful energy, economic and reduction of greenhouse gas emissions assessment of solar water heater and solar air heater for heating purposes in Gaza, Palestine. Heliyon. 2023; 9(6): e12606.
[23] Herrando M, Elduque D, Javierre C, Fueyo N. Life Cycle Assessment of solar energy systems for the provision of heating, cooling and electricity in buildings: A comparative analysis. Energy Conversion and Management. 2022; 257: 115402.
[24] Cruz T, Schaeffer R, Lucena A F, Melo S, Dutra R. Solar water heating technical-economic potential in the household sector in Brazil. Renewable Energy. 2020; 146: 1618-1639.

[25] Ahmed K, Pylsy P, Kurnitski J. Monthly domestic hot water profiles for energy calculation in Finnish apartment buildings. Energy and Buildings. 2015; 97: 77-85.

[26] Evarts J C, Swan L G. Domestic hot water consumption estimates for solar thermal system sizing. Energy and Buildings. 2013; 58: 58-65.

[27] Koiv T A, Mikola A, Toode A. DHW design flow rates and consumption profiles in educational, office buildings and shopping centres. Smart Grid and Renewable Energy. 2013; 4: 287-296.

[28] Sousa V, Meireles I. Dynamic simulation of the energy consumption and carbon emissions for domestic hot water production in a touristic region. Journal of Cleaner Production. 2022; 355: 131828.

[29] Shirinbakhsh M, Mirkhani N, Sajadi B. A comprehensive study on the effect of hot water demand and PCM integration on the performance of SDHW system. Solar Energy. 2018; 159: 405-414.

[30] Mamouri S J, Bénard A. New design approach and implementation of solar water heaters: A case study in Michigan. Solar Energy. 2018; 162: 165-177.

[31] Nkwetta D N, Vouillamoz P E, Haghighat F, El-Mankibi M, Moreau A, Daoud A. Impact of phase change materials types and positioning on hot water tank thermal performance: Using measured water demand profile. Applied Thermal Engineering. 2014; 67(1-2): 460-468.

[32] Dongellini M, Falcioni S, Morini G L. Dynamic simulation of solar thermal collectors for domestic hot water production. Energy Procedia. 2015; 82: 630-636.

[33] Bouhal T, Agrouaz Y, Allouhi A, Kousksou T, Jamil A, El Rhafiki T, Zeraouli Y. Impact of load profile and collector technology on the fractional savings of solar domestic water heaters under various climatic conditions. International Journal of Hydrogen Energy. 2017; 42(18): 13245-13258.

[34] Khavari M, Veysi F. Investigating the Effect of Hot Water Consumption Profile on the Performance of Solar Water Heating Systems. Energy Engineering and Management. 2023; 9(2): 96-105.

[35] Shafieian A, Khiadani M. Integration of heat pipe solar water heating systems with different residential households: An energy, environmental, and economic evaluation. Case Studies in Thermal Engineering. 2020; 21: 100662.

[36] Gambade J, Noël H, Glouannec P, Magueresse A. Parametric Study and Long-term Prediction of the Production of a Solar Water Heaters Installation. In E3S Web of Conferences. 2023; 433: 2004.

[37] Zukowski M, Jezierski W. New Deterministic Mathematical Model for Estimating the Useful Energy Output of a Medium-Sized Solar Domestic Hot Water System. Energies. 2021; 14(10): 2753.

[38] Oye T. K, Gupta N, Goh K, Kerrouche A, Oye T. T. Holistic Modelling and Parametric Study of Bathroom Solar Hot Water Heating System. Environmental Management and Sustainable Development. 2021; 10(3): 36-61.

[39] MATLAB Simulink R2016b. The Mathworks Inc.

[40] Solar rating and certification corporation, ICC-SRCC certification and listing directories. 2017. http://www.solar-rating.org/certification_listing_directory/index.html. Accessed 3 March 2017.

[41] Duffie J A, Beckman W A. Solar Engineering of Thermal Processes, fourth ed., John Wiley & Sons, New York, 2013.

[42] Bahadori M N, Chamberlain M J. A simplification of weather data to evaluate daily and monthly energy needs of residential buildings. Solar Energy. 1986; 36(6): 499-507.

[43] ASHRAE. ASHRAE Handbook HVAC Applications, SI ed., Service Water Heating, ASHRAE Inc., Atlanta, 2011.

[44] Russo B J, Chvala W D. American Recovery and Reinvestment Act (ARRA) Federal Energy Management Program Technical Assistance Project 281 Solar Hot Water Application Assessment for US Army IMCOM-Southeast Region. Pacific Northwest National Lab. (PNNL), Richland, WA (United States), 2010.

[45] Kulkarni G N, Kedare S B, Bandyopadhyay S. Determination of design space and optimization of solar water

heating systems. Solar Energy. 2007; 81(8): 958-968.

[46] Notton G, Motte F, Cristofari C, Canaletti J-L. Performances and numerical optimization of a novel thermal solar collector for residential building. Renewable and Sustainable Energy Reviews. 2014; 33: 60-73.

[47] Duff W. Advanced solar domestic hot water systems. International Energy Agency, Task 14. 1996.